

# Signatures of chaotic tunnelling

Amaury Mouchet\*

*Laboratoire de Mathématiques et de Physique Théorique, Université François Rabelais,  
Avenue Monge, Parc de Grandmont 37200 Tours, France.<sup>†</sup>*

Dominique Delande<sup>‡</sup>

*Laboratoire Kastler-Brossel, Université Pierre et Marie Curie, 4, place Jussieu, F-75005 Paris, France.*

(Dated: February 8, 2008)

Recent experiments with cold atoms provide a significant step toward a better understanding of tunnelling when irregular dynamics is present at the classical level. In this paper, we lay out numerical studies which shed light on the previous experiments, help to clarify the underlying physics and have the ambition to be guidelines for future experiments.

PACS numbers: 05.45.Mt Semiclassical chaos (quantum chaos)  
05.60.Gg Quantum transport  
32.80.Qk Coherent control of atomic interactions with photons  
05.45.Pq Numerical simulations of chaotic models

## I. INTRODUCTION

When studying tunnelling in non-separable systems with more than one degree of freedom, one immediately encounters difficulties which generically can be traced back to the absence of enough constants of motion. Even in the very peculiar case of integrable systems, where continuous symmetries provide as many constants of motion as degrees of freedom, as soon as separability is lost, the analysis of tunnelling is not a simple generalization of what occurs in one-dimensional (1D) autonomous systems. The later case is detailed in textbooks on quantum physics (see for instance [1]) and it has even been possible to give a comprehensive analytical treatment in term of complex solutions of the Hamilton equations [2]. However, it is not until the mid-eighties that a satisfactory quantitative approach has been proposed [3, 4] for tunnelling in non-separable integrable systems involving a larger number of dimensions. Moreover, integrability is a property of higher dimensional systems which is not generic. The coupling between several internal degrees of freedom as well as the coupling to an external source usually destroys some global constants of motion. With such a lack of constraints on the dynamics, the classical motion in phase space may become chaotic: it may explore volumes with higher dimensionality and therefore becomes exponentially sensitive on initial conditions. It is not surprising that these deep qualitative differences between an integrable regime and a chaotic one appear at the quantum level too. Some of the properties of a *quantum* system do change when constants of motion are broken and, indeed, it is the very object of quantum chaos to study the signatures of classical chaos at

the quantum level (see for instance [5] to see how rich, vivid and successful this domain is).

We define tunnelling as a quantum process which is classically forbidden to *real* solutions of classical equations of motion. In this paper, we consider Hamiltonian systems only and study how the non-dissipative breakdown of continuous symmetries affects tunnelling. We do not consider how tunnelling is modified by dissipation and decoherence of the quantum wave. Of course, this requires a great care in real experiments where making dissipation negligible is always a hard task. This is one of the main reasons why very few real experiments have been done on these questions, though they would definitely help to understand tunnelling in the presence of chaos (as far as we know, the only experiments explicitly made on chaotic tunnelling in the XX<sup>th</sup> century are those presented in [6] with electromagnetic microwaves instead of quantum waves).

During the last fifteen years however, theoretical and numerical investigations on autonomous 2D and time-dependent 1D Hamiltonians systems highlighted some mechanisms [3, 4, 7, 8, 9, 10, 11, 12] and much insight has been gained on the influence of non-separable dynamics. Experimental evidence of such mechanisms would be of great interest especially in the light of the subtle interplay between interferences and disorder. These phenomena lie in the general context of wave transport in complex media where the role of disorder is played by the (deterministic) chaotic dynamics instead of having a statistical random origin. Of course, other important motivations can be found in the numerous domains where tunnelling plays a crucial role as a fundamental quantum process like ionization [13], absorption, nuclear radioactivity, molecular collisions, mesoscopic physics etc. More speculatively, studies on tunnelling in high dimensional Hamiltonian systems should provide us with a natural extension of the instanton techniques which deal with quantum field theories reducible to effective 1D autonomous Lagrangian systems.

---

\*Electronic address: mouchet@celfi.phys.univ-tours.fr

<sup>†</sup>URL: <http://www.phys.univ-tours.fr/~mouchet>

<sup>‡</sup>Electronic address: delande@spectro.jussieu.fr

In 2001, it has been shown both theoretically [14] and experimentally [15, 16, 17, 18] that atom cooling techniques [19] (and possibly molecular physics as well, where formally similar systems have been extensively studied [20, 21, 22, 23]) provide systems which fulfill all the severe requirements to study tunnelling in the presence of classical Hamiltonian chaos: accurate manipulation of internal and external degrees of freedom, precise control of dissipation and decoherence and on the preparation/detection set up. For a brief account intended for a large audience see [24, 25, 26]). The present article has the ambition to mark out the future challenging experiments, that remain to be done for reasons which will hopefully appear clear in the following.

This paper is organised as follows. In section II we give a general and informal overview. In section III, we quickly recall the main theoretical apparatus that is needed in the following. We implicitly refer to [14] for details and demonstrations. In section IV, we comment the results of [15] and [16]. In section V, we show in this context, with the help of numerical experiments, the very precise form taken by the phenomenon known as chaos assisted tunnelling. We explain why it has not been observed yet with real atoms and propose how to actually bring it to the fore. Before the concluding remarks in section VII, we give in section VI some more numerical results which illustrate how subtle the signatures of chaotic tunnelling can be.

## II. CHAOTIC TUNNELLING

The simplest situation to illustrate tunnelling is probably the case of a particle placed in a 1D time-independent symmetric double-well potential (see Fig. 1 (a)). Starting in one well with an energy that is below the maximum of the potential, a quantum particle can jump into the other well with a non zero probability though it is a forbidden classical process. In addition to the classical time scale  $\tau$  given by the oscillating period *inside* one well, we therefore have a longer time scale, the tunnelling period  $T \gg \tau$  of the oscillations *between* the wells. In the eigenenergy spectrum, tunnelling appears as a quasi-degeneracy of the odd and even-symmetry states whose energies are both of the order of  $\hbar/\tau$  but differ by an exponential energy splitting

$$\Delta\epsilon = \frac{2\pi\hbar}{T} \sim e^{-A/\hbar} \quad (1)$$

where  $A$  is a  $\hbar$ -independent typical action and can be interpreted in terms of a unique complex classical trajectory under the barrier [1, 27].

In the following we generalize this elementary situation in two ways. First, unlike the parity in the previous example, we can deal with a symmetry which is not necessarily either a spatial one or a two-fold one. In other words, we can have any discrete symmetry group acting on the whole phase space as well as any  $N$ -fold

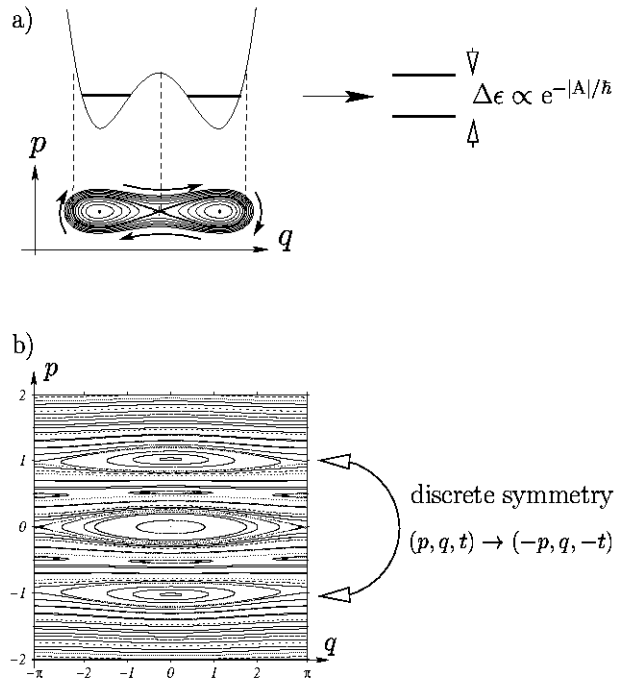


FIG. 1: A generalization of the paradigmatic double well potential (a) is to consider tunnelling between stable islands that are related by any discrete symmetry in phase space. Case (b) corresponds to Hamiltonian (2) with  $\theta = 1$  and  $\gamma = 0.018$ . Here, the time reversal symmetry plays the role of parity in case (a).

symmetry which lead to bunches of  $N$ -uplets in the energy spectrum (or bands if  $N \gg 1$ ). In the following we keep  $N = 2$  since we have a two-fold symmetry  $\mathcal{T}$  actually playing the role of parity (see Fig. 1 (b)) and being somehow decoupled from the other discrete symmetries. The classical structure in phase space is globally invariant under  $\mathcal{T}$  and the quantum eigenstates can be classified according to their symmetric or antisymmetric character under the unitary transformation which represents  $\mathcal{T}$  in the Hilbert space of states. Because  $\mathcal{T}$  acts in phase space, it is usually more complicated than a pure spatial transformation. Thus, the two regions of phase space connected by *quantum* tunnelling, but *classically* not connected, are in general not separated by a simple potential barrier, but by a more complicated dynamical barrier. In such a case, tunnelling is emphasized to be called “dynamical tunnelling” as suggested by Davis and Heller in [28]. It often happens that the classically unconnected region are associated to the same region of configuration space, with different momenta. A simple study of the density probability in configuration space is then insufficient to characterize dynamical tunnelling; an analysis of the density probability in momentum space is required.

The second kind of generalization leads to much more puzzling questions. When dealing with systems with sev-

eral degrees of freedom or, equivalently, if an external time dependence exists, classical trajectories generically lose their regular behavior, cannot analytically be computed and are organized in a fractal hierarchy that is described by the KAM perturbative scenario. Recently, important progress has been achieved in the understanding of the continuation of these intricate structures in complex phase space and their role at the quantum level, see [29, 30] and especially [31]. Anyway, we are therefore led to the following typical quantum chaos question: if one is able to create two symmetric stable islands separated in classical phase space by a chaotic sea whose volume is under control (see Fig. 2), what is the effect of this sea on the (dynamical) tunnelling between the islands?

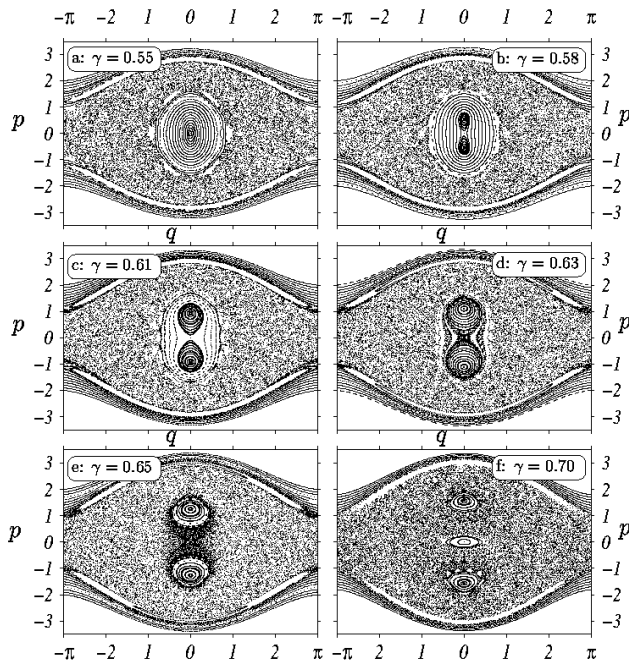


FIG. 2: Poincaré surfaces of section correspond to Hamiltonian (2) with  $\theta = 1.724137$ . Two stable islands in the vicinity of the origin are created by a pitchfork bifurcation at  $\gamma \simeq 0.56$ . Above this value, chaotic motion progressively invades phase space in between the two stable islands. At  $\gamma > \gamma_c \simeq 0.625$ , the latter are no longer connected by regular trajectories. The experimental configuration used in the NIST experiments corresponds to  $\gamma = 0.96$  just before the islands disappear in a bifurcation cascade at  $\gamma \simeq 0.97$ .

The “dual” situation where chaos is created *inside* the wells while the dynamical barrier is kept regular has been introduced and studied theoretically and numerically in [11]. For a better understanding of what occurs in the energy spectrum when regular wells are separated by a chaotic sea, it has been proposed in [32] to slightly break the tunnelling symmetry. Nevertheless, in the following of the present paper, it must be kept in mind that

a discrete symmetry will be always maintained exactly. At last, a third kind of generalization where the Hamiltonian character is destroyed by introducing dissipation and/or coupling to a thermal bath, is beyond the scope of this work [33].

### III. EFFECTIVE HAMILTONIAN SYSTEM

Following [14, 15, 16] (see also [34] in a different context) we deal with an effective 1D time-dependent system whose Hamiltonian is

$$H(p, q; t) = \frac{p^2}{2} - \gamma (\theta + \cos t) \cos q \quad (2)$$

in dimensionless units.  $\gamma$  and  $\theta$  are two classical real parameters that can be modified in real experiments. In addition, there is also one parameter, namely  $\hbar_{\text{eff}}$ , which fixes the quantum scale and is defined by the usual relation between canonical operators:  $[q, p] = i\hbar_{\text{eff}}$ . It turns out that  $\hbar_{\text{eff}}$  is not constant any longer (see section IV below). It can be also experimentally varied via the rescaling factor that is needed in the canonical commutation relation in order to work in dimensionless units used to write (2).

The time dependence breaks the conservation of energy and therefore may generate chaos. In order to deal with such a Hamiltonian, it is crucial to remark that it has both a spatial and a temporal periodicity. The latter implies that the Floquet theorem can be used, which states that the Hilbert space is spanned by an orthonormal eigenbasis of the evolution operator over one period. The corresponding eigenvalues of this unitary operator are distributed on the unit circle and therefore are labelled by their phase, which is conveniently written as  $\exp(i2\pi\epsilon/\hbar_{\text{eff}})$ , where  $2\pi$  stands for the period of the modulation and  $\epsilon$  can be interpreted as a quasi-energy, a generalization of the notion of energy level for a time-periodic system.

The spatial periodicity of the Hamiltonian is also extremely important, as it makes it possible to split the Hilbert space into independent components, each component being characterized by the so-called Bloch vector  $k$  in the  $]-0.5, 0.5]$  range: under translation of  $2\pi$  along  $q$ , the quasi-energy eigenstates are just multiplied by the phase factor  $\exp(i2\pi k)$ . One is thus reduced to solve the Floquet-Schrödinger equation in an elementary spatial cell with boundary conditions depending on  $k$ . One thus generates – for a fixed value of  $k$  – a discrete quasi-energy spectrum  $\epsilon_i(k)$ . When the full range of  $k$  values is considered, one obtains the familiar (quasi-)energy bands [35].

There is an additional discrete symmetry which can be used. The Hamiltonian (2) is invariant under the time-reversal symmetry  $(q, p, t) \rightarrow (q, -p, -t)$ . In the classical surfaces of section, this implies a symmetry with respect to the  $q$  axis. In situations like the one in fig. 1b, this implies the existence of pairs of symmetric classically unconnected tori, i.e. a situation where tunnelling could be

observed. In the quantum world, the situation is slightly more complicated, because this symmetry connects the  $k$  subspace to the  $-k$  subspace. In the particular case  $k = 0$  ( $k = 0.5$  could also be used), this implies that the Floquet eigenstates can be split in two subclasses of states which are either even or odd under the symmetry operation. The splitting between a doublet of even and odd states,  $\Delta\epsilon_n = |\epsilon_n^+(0) - \epsilon_n^-(0)|$  will be a measure of tunnelling.

We will extensively use the Husimi representation of a quantum state [36]. Such a representation associates to each quantum state  $|\psi\rangle$  a phase space function  $\psi^H(p, q)$  (where  $p$  and  $q$  are real numbers) defined by

$$\psi^H(p, q) = |\langle z|\psi\rangle|^2 \quad (3)$$

where  $|z\rangle$  is the coherent state corresponding to the complex number  $z = (q + ip)/\sqrt{2\hbar_{\text{eff}}}$ . Because  $|z\rangle$  is a minimal Gaussian wave packet with average momentum  $p$  and average position  $q$ , the Husimi function  $\psi^H(p, q)$  contains some information about the degree of localization of  $|\psi\rangle$  in phase space, and makes it possible to associate quantum states with classical phase space structures.

#### IV. EXPERIMENTS WITH COLD ATOMS

Under some severe conditions which constrain the experiments, Hamiltonian (2) can be obtained as an effective dimensionless Hamiltonian for cold neutral independent atoms of mass  $M$  interacting with two counterpropagating laser beams [14, 15, 16]. These two beams have two slightly different frequencies at  $\omega_L + \delta\omega/2$  and  $\omega_L - \delta\omega/2$ . The longitudinal coordinate  $x$  and the dimensionless  $q$  are related by  $q = 2k_L x$  where  $k_L = \omega_L/c$ . The rescaling of the momentum is given by  $p = (2k_L/M\delta\omega)p_x$ .  $\gamma$  and  $\theta$  are fixed by the intensity of the lasers and the detuning of the laser frequencies with respect to the atomic resonance. The dimensionless time  $t$  is taken in  $\delta\omega^{-1}$  units and the expression of the effective Planck constant is  $\hbar_{\text{eff}} = 8\omega_R/\delta\omega$  where  $\omega_R = \hbar k_L^2/2M$ . Since *in fine* we want to measure exponentially small tunnelling splittings  $\Delta\epsilon$ , it requires to maintain these conditions for a time at least larger than  $\hbar_{\text{eff}}/\Delta\epsilon$ . Moreover, a very accurate control of the preparation of the initial state and of the analysis of the final state is compulsory.

As shown above, because of the temporal and spatial periodicity of the Hamiltonian, observing the standard signature of tunnelling, that is an oscillation of a quantum state between two classically unconnected regions of phase space requires that a single doublet of Floquet-Bloch eigenstates is initially populated, with well defined values of the parameters  $(\gamma, \theta, \hbar_{\text{eff}})$  but also with a well defined value of the Bloch angle  $k$ . If more than a single doublet is populated, additional frequencies (related to energy differences between the various populated Floquet states) will appear in the temporal evolution. If any parameter is not fixed, the experimental signal will

be the superposition of tunnelling oscillations (with different frequencies) for various sets of parameters. This will at best – if the dispersion of the parameter values is reasonably small – blur the oscillations at long time and at worst will completely destroy the signature of dynamical tunnelling. It is experimentally rather simple to keep an accurate time-periodicity of the driving signal, i.e. to fix  $\hbar_{\text{eff}}$ . Similarly, the balance between the constant and the oscillatory term, hence the parameter  $\theta$  is easily controlled. The  $\gamma$  parameter is proportional to the laser intensity and may thus slightly vary across the atomic cloud (because of the transverse structure of the laser beams). The most difficult part is to control that a single Bloch angle  $k$  is excited. Indeed, this requires a phase coherence of the initial wavefunction over a large number of laser wavelengths, which is extremely difficult to achieve experimentally [37], as will be shown in the following. In any case, the inhomogeneous broadening of the experimental signal because of the dispersion in  $k$  will be responsible for a decay of the tunnelling oscillations.

#### A. NIST experiments [15]

In the NIST experiments, the two stable symmetric islands are chosen quite close in phase space in order to deal with not too small splittings. Another crucial point of this experiment is that the classical motion of the islands over one period, unlike those in [14] and [16], always remains trapped in one spatial elementary cell of length  $2\pi$ . The quantum states localized in these islands are consequently only weakly sensitive on the boundary conditions which are governed by the Bloch angle. In other words, the tunnelling period will be only weakly dependent on the Bloch angle  $k$ , which implies that the unavoidable broadening over  $k$  will not spoil too much the signature of tunnelling. This is a major improvement over the tunnelling described in [14] and [16], where a very narrow band of Bloch angle is required to observe clear tunnelling oscillations. Moreover, the atoms involved in the tunnelling process stay longer in the region where the laser intensities are uniform.

Indeed, as proposed in [38], [17, chap. 4 and 5] the two stable symmetric islands are created from a pitchfork bifurcation of the fixed point at  $(p, q) = (0, 0)$ . To visualize it (see Fig. 2 (a) and (b)), we extract a one-parameter sequence by varying  $\gamma$  while  $\theta$  is fixed to the experimentally chosen value in [15], i.e.  $\theta = 1.7$ . When  $\gamma$  is increased, the pairs of symmetric tori appear at  $\gamma \simeq 0.56$ . At the center of each set of tori, there is a periodic orbit. Over one period of the driving, the periodic orbit is essentially a rotation over the fixed point at  $(p, q) = (0, 0)$ , which explains that the whole structure remains trapped in a single spatial cell. For  $0.56 \lesssim \gamma \leq \gamma_c$ , the tori remain nested in one connected stable island. At  $\gamma = \gamma_c \simeq 0.625$ , a chaotic sea separates the symmetric islands which shrink and move away from the central point before being dissolved through a cascade of bifur-

cations starting at  $\gamma \simeq 0.97$ .

In one series of experiments,  $\gamma \simeq 0.96$  and  $\hbar_{\text{eff}} \simeq 0.8$ , the atoms are prepared in one island and their average momentum  $\langle p \rangle$  is measured stroboscopically every modulation period ( $= 2\pi$  in dimensionless units). Since, in phase space, the islands rotate about the origin with the same period, if no tunnelling occurred no variation in  $\langle p \rangle$  would be noticeable. In fact, starting the measurement sequence when  $\langle p \rangle$  has its maximum value, oscillations are observed which illustrate the back and forth motion of the atoms between the islands due to dynamical tunnelling. The tunnelling period  $T$  is about 10 modulation periods in this case (200  $\mu\text{s}$ ). This is in perfect agreement with the quasi-energy splitting obtained numerically for the two Floquet eigenstates having the largest Husimi functions inside the islands.

It is worth noting that the NIST group uses a Bose-Einstein condensate as a preliminary step for preparing atoms in well defined quantum states, especially for achieving a large coherence length for the wavefunction, i.e. a small spreading of the Bloch angle  $k$ . In order to prepare phase space localized states, an optical lattice is carefully turned on. When the tunnelling experiment starts, the atomic density and the interaction between atoms is sufficiently small, and the experiment can be analyzed as the interaction of individual independent atoms with the laser beams, i.e. using Hamiltonian (2). However, the cloud of atoms remains cold enough, at a sub-recoil temperature, to prevent a large thermal broadening of momentum distribution that would destroy the signal. Because they start from very low temperature, these preparation techniques based on condensate manipulation seem to allow a wider room to manoeuvre than those working with thermal clouds only. Adiabatic switching of the light potentials is not required and one can actually work with values of the classical parameters  $\gamma$  and  $\theta$  which are far from the perturbative regime of an integrable system.

By diagonalizing the evolution operator corresponding to eq. (2) over one period, we are not only able to reproduce the oscillatory behavior of  $\langle p(t) \rangle$  (see Fig. 3 (a)), but also we can study the spoiling effect of the thermal dispersion  $\Delta p \propto \sqrt{\text{temperature}}$  and predict the maximum allowed temperature (see Fig. 3 (b) and (c)).<sup>1</sup> If  $\alpha$  denotes the width of the momentum distribution in recoil momentum units, it can be shown [14, §6.a] that it corresponds to a statistical mixture of Bloch states with  $\Delta k = \alpha/2$ . Fig. 3 (a) corresponds to the ideal situation where all atoms are prepared with  $\alpha \ll 1$  about the

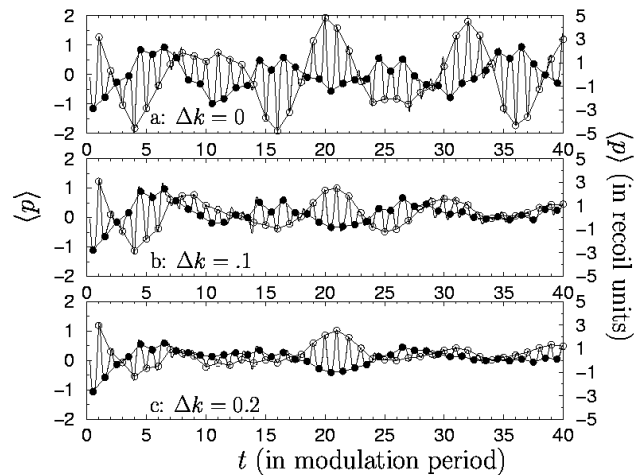


FIG. 3: Numerical simulation of the quantum evolution, in the conditions of the NIST experiment, i.e.  $\theta = 1.72$ ,  $\gamma = 0.96$  and  $\hbar_{\text{eff}} = 0.8$  (compare to Fig. 4 (a) of [15]). Starting at  $t = 0$  with a Gaussian wave packet whose Husimi function is localized in one stable island (with a vanishing average momentum), we follow the average momentum  $\langle p \rangle$  as time evolves. The stroboscopic measurements at times  $\pi + 2m\pi$  (resp.  $3\pi + 2m\pi$ ) with  $m \in \{0, 1, \dots, 40\}$ , are plotted with the white (resp. black) circles. The tunnelling oscillations are clearly visible; the tunnelling period can be extracted from the typical time scale of the envelop: it is about 10 modulation periods. In the upper plot (a), we assume that a single Bloch angle  $k = 0$  is initially prepared (which implies a perfect phase coherence of the wavefunction across the optical lattice). The (thermal) dispersion of the Bloch angle washes out the signal: in case (b), we take a momentum distribution with width  $\Delta p = \alpha = 2\Delta k = 0.2$  and in case (c)  $\Delta p = 0.4$ . In the latter case, the amplitude of the envelopes are so weak that this corresponds to an upper bound in temperature (about 1/5th of the recoil temperature) at which tunnelling can be measured.

$k = 0$ . When a small but non vanishing  $\alpha$  is introduced, some states of the quasi-energy bands with non vanishing  $k$  get involved and blur the tunnelling oscillations. For  $\alpha = 0.2$ , the oscillation amplitude is reduced by a factor 2 and for  $\alpha = 0.4$  have nearly disappeared. Therefore, in this experiment, having a sub-recoil atom cloud is required.

In the following we want to focus on tunnelling only and we will implicitly keep  $k = 0$ .

## B. Austin experiments [16]

For a better understanding of the dynamics, one must go beyond the two-level model involving the symmetric and the antisymmetric states only. Other states must be taken into account and their influence can be enlightened when a classical parameter ( $\gamma$  or  $\theta$ ) or the quantum one ( $\hbar_{\text{eff}}$ ) is continuously varied. Two (quasi-)energies may exactly get degenerate if they belong to distinct symme-

<sup>1</sup> After the first version of the present paper was written, we learnt that an independent numerical work [39] had obtained the same results as the ones in our Fig. 3 (a). But [39] do not consider the thermal effects and work always within the Floquet theory at  $k = 0$  instead of the Floquet-Bloch theory. In the present work we clearly demonstrate that thermal effects cannot be neglected and must be studied carefully when experiments are discussed.

try classes. If not, they may follow a so-called avoided crossing whose size reflects the direct coupling between the two states (more precisely the off-diagonal matrix element of the coupling perturbation), but also the indirect coupling with other states. One of the keys of the chaotic tunnelling problems is to identify clearly the qualitative nature and the quantitative influence of indirect coupling. This is the background of Austin experiments.

A third level is involved in a non negligible indirect coupling when its quasi-energy approaches the tunnelling doublet energies. This can be understood from perturbation theory as the leading term of the indirect coupling is proportionnal to the inverse of the energy difference. The two generic scenarii of the crossing of the doublet by a third state are shown in Fig. 4. Aside from the

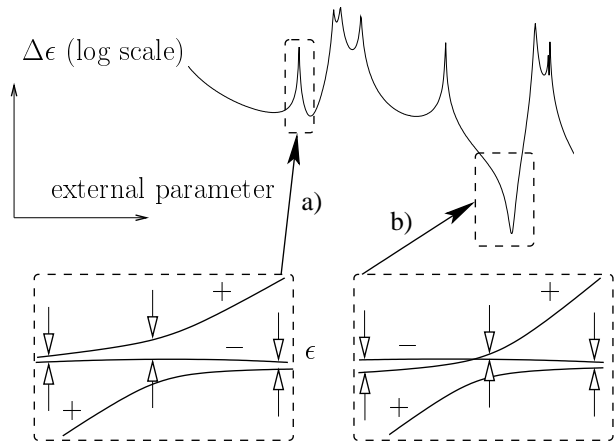


FIG. 4: When a third level is crossing a tunnelling doublet when a parameter of the Hamiltonian is varied, there is an avoided crossing between the third level and the member of the doublet with the same symmetry, while the other member of the doublet (with opposite symmetry) ignores the third level. Two generic scenarii exist: in case (a), the tunnelling splitting increases in the vicinity of the avoided crossing; in case (b), it decreases and vanishes at a specific value of the parameter.

unavoidable ambiguous definition of the splitting, it appears clearly that case a) corresponds to an increase of the tunnelling splitting during the crossing while, conversely, case b) can lead to arbitrary small splittings since an exact degeneracy occurs. Thus, such a crossing by a third state produces a sharp variation of the tunnelling period that can be measured experimentally. This is actually what is observed in the Austin experiments and can be confirmed by numerical experiments as shown in Fig. 5. When looking at the Husimi representation of the states, Fig. 6, one can immediately distinguish between the tunnelling doublet and the third state sufficiently far from the crossing. As expected, the tunnelling doublet has Husimi representations localized in the stable islands though they also spread in the chaotic sea. On a classical Poincaré surface of section, it is easy to

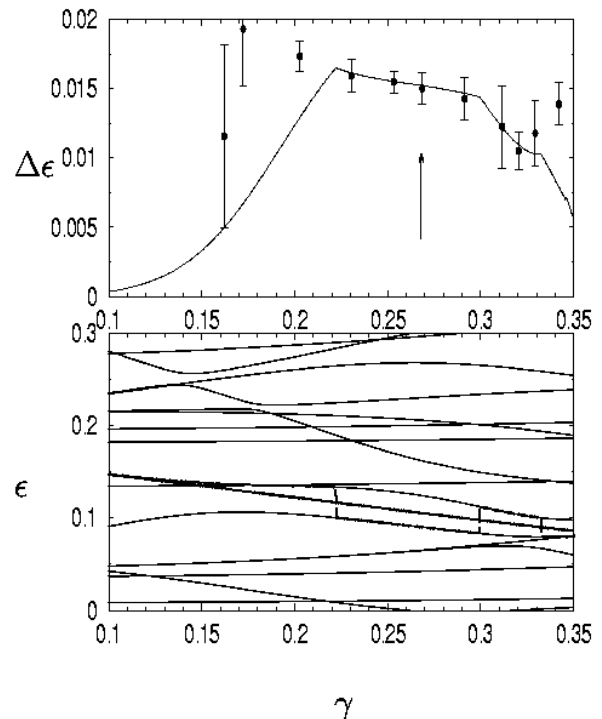


FIG. 5: Numerical results obtained with the parameters of the Austin experiment, that is Hamiltonian (2), with  $\theta = 1$  and  $\hbar_{\text{eff}} = 0.33$ . The lower plot shows a part of the quasi-energy spectrum when  $\gamma$  is varied. Thick lines show the two quasi-energies whose difference is the tunnelling splitting plotted in the upper plot. The two states are selected to have the largest localization of the Husimi function at the center of the stable islands. When a third level couples to the state that belongs to the same symmetry class, an avoided crossing can be seen and the definition of the doublet becomes necessarily ambiguous. There, some discontinuity in the selected state (and in the slope of the tunnelling frequency) cannot be avoided. The tunnelling splitting is shown as a function of  $\gamma$  in the upper plot, and is compared with the experimental results from ref. [16]. The agreement is very good, which validates the numerical approach. Around  $\gamma = 0.2$ , a discrepancy is visible. This is precisely the “ambiguous” region where the dynamics cannot be reduced to a simple tunnelling oscillation, but at least three levels must be taken into account, leading to several relevant energy splittings.

make the difference between chaotic and regular motion; how to transpose this distinction at the quantum level is not known with the large values of  $\hbar_{\text{eff}}$  used in both the Austin and the NIST experiments. Some classical structures much smaller than the de Broglie wavelength are possibly present in some of the states<sup>2</sup>, but just looking

<sup>2</sup> From time to time, it is claimed [40] that a simple matching between classical structures and quantum wave sub-Planckian structures was found but, as it was understood long time ago

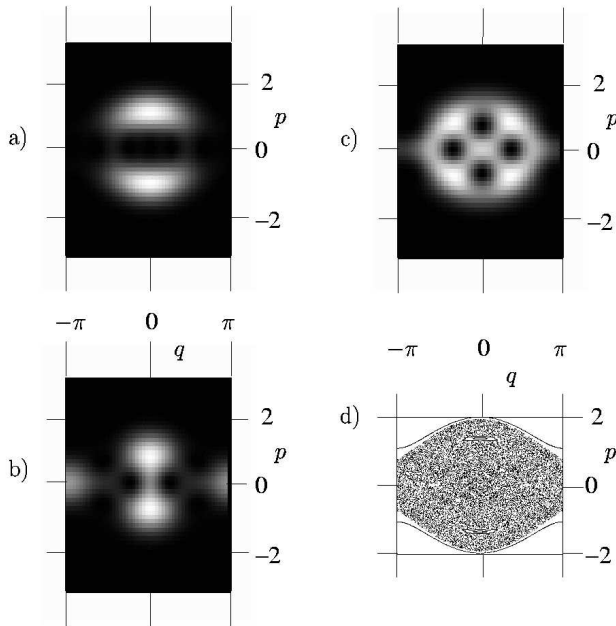


FIG. 6: (a), (b) and (c) show the density in gray scale of the Husimi functions associated with the three states which play an important role for tunnelling at  $\gamma = 0.25$  (parameters of the Austin experiment, as in fig. 5). As expected, the two members of the doublet, (a) and (b) have their Husimi function localized about the two symmetric islands visible in the classical Poincaré surface of section (d). (b) is strongly coupled to a third state shown in (c).  $\hbar_{\text{eff}}$  is too large to attribute any regular/chaotic character to the third state. (c) clearly plays a role in the enhancement of the tunnelling splitting through an indirect coupling; this is thus a “assisted tunnelling” mechanism, which cannot be unambiguously characterized as chaos assisted.

at the Husimi representation of the third state for  $\hbar_{\text{eff}} \simeq 1$  does not make it possible to attribute any chaotic or regular character to it. It is only for much smaller  $\hbar_{\text{eff}}$  that chaotic or regular wavefunctions make sense. This is not surprising: the dichotomy between regular and irregular motion is a classical one and, at present, it can be extrapolated at the quantum level within the semiclassical regime only. Anyway, one must keep in mind that tunnelling does only make sense in the semiclassical regime as well. One of the great merit of Austin experiments is to show for the first time a quantum tunnelling effect where an indirect process is involved, but we fill exaggerated to attribute any chaotic origin to it.

---

by [41], the latter are generally washed out as soon as one try to measure global averages.

## V. NUMERICAL EVIDENCE OF A CHAOTIC TUNNELLING REGIME

It is one of the first success of quantum chaos to have shown that the energy levels of an integrable system ignore each others because they are localized on different classical tori, while in chaotic systems level repulsion is the rule. Following the discussion in the previous section, one may therefore expect that the average size of avoided crossings is increased when chaos is present. The fluctuations of a tunnelling process which should be narrow and sparse in an integrable regime should be broader, more numerous and possibly involving many states in a chaotic regime. We now illustrate this statement in the framework of the experimental atomic Hamiltonian (2).

There are two different ways of rendering chaos observable by quantum eyes: the first one consists in increasing the volume of the chaotic sea with the help of a classical parameter, the other one fixes the classical dynamics and decreases  $\hbar_{\text{eff}}$ . We will present both ways.

**CAT, RAT and all that...** One may try to study the tunnelling *fluctuations* separately from the *average behavior*. This average — in a somewhat vague sense — is increased because chaos diminishes the classical dynamical barrier<sup>3</sup> and this is the reason why the phenomenon can be called chaos assisted tunnelling. However, as far as only fluctuations are concerned (there can be an enhancement or a decrease as well), the words “chaos assisted tunnelling” (CAT) [10] may lead to confusion and we simply use “chaotic tunnelling”. At last, Brodier, Schlagheck and Ullmo discovered what they called “resonant assisted tunnelling” (RAT) [42] to describe an enhancement of tunnelling due to an indirect process which involves one or several quasi-modes localized in the secondary resonances surrounding the main symmetric islands. Up to now, RAT has been studied quantitatively in a purely quasi-integrable case but there are clues that it can be extended far beyond KAM theory.

### A. $\gamma$ change

Let us first take  $\hbar_{\text{eff}}$  ten times smaller than in the NIST and Austin experiments. It is much easier to do it numerically than experimentally, as it requires to increase the modulation frequency of the laser beams by one order of magnitude. We then follow the quantum states through the classical bifurcation shown in picture 2 and discussed in section IV A. Again, in order to calculate the tunnelling splitting  $\Delta\epsilon$ , we select the states that have the

---

<sup>3</sup> The question of defining an integrable system with respect to which the chaotic one should be compared is extremely difficult because of the exponential sensitivity of tunnelling on classical parameters. It is a much more serious problem than the way of defining an averaging procedure.

largest Husimi functions inside the islands.

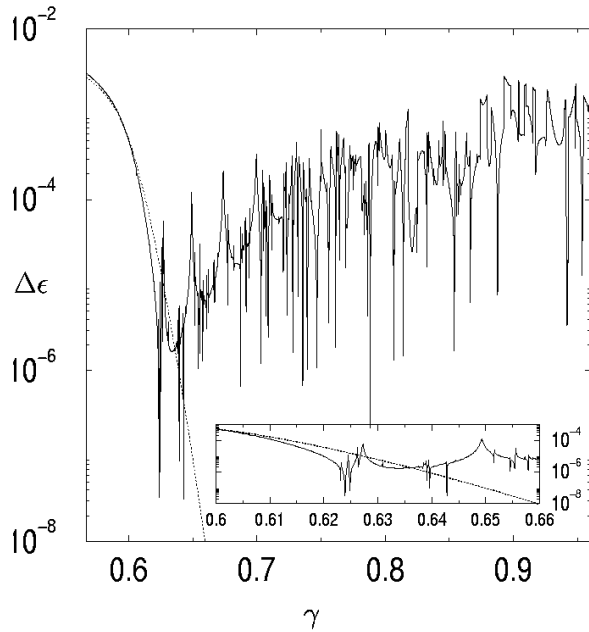


FIG. 7: The tunnelling splitting as a function of  $\gamma$ , for  $\theta = 1.724137$  and  $\hbar_{\text{eff}} = 0.079638$ , that is 10 times smaller than in the NIST experiments. Two regimes are clearly separated by the critical value  $\gamma_c \simeq 0.625$ ; these two *quantum* regimes correspond to two different *classical* regimes in the Poincaré surfaces of section in Fig. 2. The smooth average decrease with sparse and narrow fluctuations ( $\gamma < \gamma_c$ ) corresponds to the case where the symmetric classical tori belong to the same regular island. The Hamiltonian can there be approximated by a simple integrable Hamiltonian, using the normal form described in the appendix. The dotted line corresponds to the splitting calculated with this normal form and is in good agreement with the numerical result. In the second regime ( $\gamma > \gamma_c$ ), there are huge quantum fluctuations of the tunnelling splitting (and a slightly increased average value). Classically, this corresponds to tunnelling between unconnected symmetric islands, separated by a chaotic sea.

Figure 7 shows that, after a smooth decrease of  $\Delta\epsilon$  up to  $\gamma = \gamma_c \simeq 0.625$  there is an abrupt change of regime. First, the mean value of  $\Delta\epsilon$  increases and second, many fluctuations appear which modify the splitting by several orders of magnitude. It is remarkable that this change of regime can be matched on the Poincaré surfaces of section. The smooth tunnelling regime occurs the resonant tori belong to one quasi-integrable island. For  $\gamma < \gamma_c$ , we are able to reproduce the main features of tunnelling by using an integrable approximation (see appendix). The decrease of tunnelling is directly understood in terms of the lengthening of the dynamical barrier.  $\gamma_c$  corresponds exactly to the point where the islands get disconnected. In addition, one can follow the bifurcation on the Husimi representations of the tunnelling doublet.

One can hardly detect by eye any regularity in the chaotic regime but four large spikes in the range  $\gamma_c <$

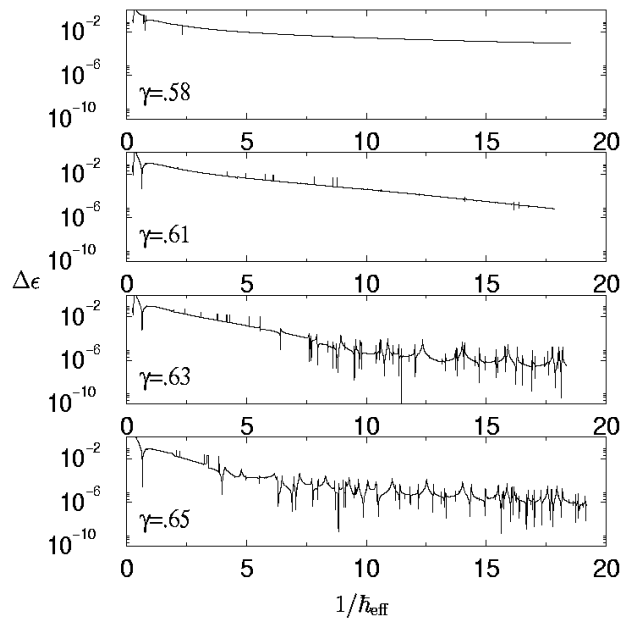


FIG. 8: The tunnelling splitting as a function of  $\hbar_{\text{eff}}$ , for fixed values of the classical parameters, i.e. fixed classical dynamics ( $\theta = 1.724137$  and four values of  $\gamma$ ). In the regular regime, an exponential decrease, as described by eq. (1) is visible, as a straight line with a negative slope in a logarithmic scale. The regime of fluctuations can be seen for  $\gamma > \gamma_c$  when  $\hbar_{\text{eff}}$  is small enough for the de Broglie wavelength to be comparable to the size of the chaotic sea between the two islands.

$\gamma < 0.7$ . This can be traced back to the crossing by the same third state whose quasi-energy line is folded four times in the Floquet zone centered on the doublet.

### B. $\hbar_{\text{eff}}$ change

Figure 8 shows  $\Delta\epsilon$  as a function of  $1/\hbar_{\text{eff}}$  for four values of  $\gamma$ . Here again, two types of regimes, a quasi-regular and a chaotic one, can clearly be distinguished. For the values of  $\gamma$  where some substantial chaos is present in between the islands, by decreasing  $\hbar_{\text{eff}}$ , one gets to the chaotic regime. For  $\gamma < \gamma_c$ , i.e. in the quasi-regular regime, one may enter in a chaotic regime but for far much low value of  $\hbar_{\text{eff}}$  since the chaotic layers between KAM tori are so thin that they are not even resolved in the Poincaré surface of section given in the figures.

On this plots, a purely exponential law given by eq. (1) would produce a straight line with negative slope. It gives rather poor predictions in the chaotic regime and should be corrected even in the quasi-integrable regime in order to reproduce the fluctuations. Whenever such a fluctuation is due to a crossing by a quasi-mode (and not a state delocalized in the surrounding chaotic sea), it might be reproduced by the resonance assisted tunnelling techniques.



## VI. STATISTICAL SIGNATURE OF CHAOTIC TUNNELLING ?

In order to reproduce quantitatively the statistics of the tunnelling splitting fluctuations in the chaotic regime, Leyvraz and Ullmo [43] have introduced a random matrix model. The Hamiltonian can be split in two uncoupled components associated with the two even and odd symmetry subspaces. The corresponding matrices are written as:

$$H^{\text{even}} = \begin{pmatrix} \epsilon_0^+ & v_1^+ & v_2^+ & \cdots \\ v_1^+ & & & \\ v_2^+ & & H_{\perp}^+ & \\ \vdots & & & \end{pmatrix} \quad (4)$$

and

$$H^{\text{odd}} = \begin{pmatrix} \epsilon_0^- & v_1^- & v_2^- & \cdots \\ v_1^- & & & \\ v_2^- & & H_{\perp}^- & \\ \vdots & & & \end{pmatrix} \quad (5)$$

where  $\epsilon_0^{\pm}$  represent the energies of the doublet,  $H_{\perp}^{\pm}$  the Hamiltonian in the chaotic sea (modelled by a random Gaussian matrix) and  $v$  the indirect coupling.

Neglecting direct tunnelling consists in taking  $\epsilon_0^+ = \epsilon_0^-$ . The central hypothesis is to consider all the  $v$ 's as independent variables with *the same* Gaussian distribution. This is quite natural to treat all the other states on the same footing, as they are assumed to be chaotic states randomly delocalized in the chaotic sea. With these assumptions, the splitting distribution can be calculated and is given by a (truncated) Cauchy distribution, see [43]. For Hamiltonian (2), in each chaotic case where it has been tested, the Leyvraz-Ullmo prediction is in agreement with the numerical results (see [14]). More surprisingly, we have found that the Leyvraz-Ullmo law gives correct predictions even when the classical dynamics is quasi-integrable (see Fig. 9 and the corresponding Poincaré surface of section in Fig. 1) and the de Broglie wavelength much larger than the chaotic layers. When looking at the splitting, one observes numerous and large fluctuations (over several orders of magnitude) which were supposed to characterize the chaotic regime. Conversely, we have not been able to find a regular regime of fluctuations with a classically chaotic dynamics. Therefore one must conclude that even though two different regimes of tunnelling fluctuations can be identified unambiguously, classical chaos appears to be a sufficient but not a necessary condition for having numerous and large fluctuations governed by the Leyvraz-Ullmo law.

These unexpected results are not explained at the present state of the theoretical approaches of chaotic tunnelling. If it appeared, within future numerical or real experiments, that these results are not due to the peculiar properties of our system, it would definitely mean that theoretical studies should be all the more needed.

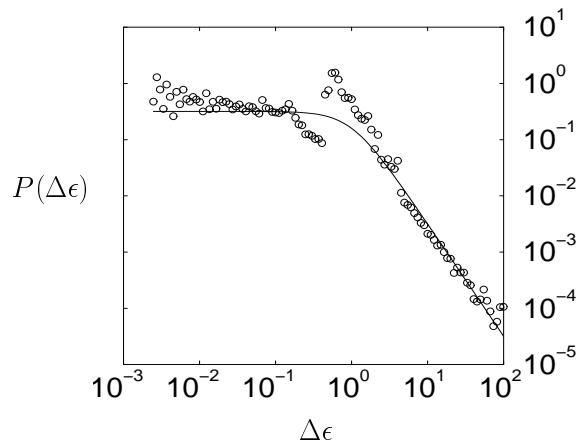


FIG. 9: Statistical distribution of the tunnelling splittings as  $\hbar_{\text{eff}}$  is varied in the quasi-integrable case corresponding to Fig. 1 (b) ( $\theta = 1$ ,  $\gamma = 0.018$ ). Surprisingly, the numerically observed distribution (small circles) is in good agreement with the Leyvraz-Ullmo law (solid line) which is supposed to be valid in the chaotic case, as it treats all the states coupled to the tunnelling doublet on the same footing. This clearly indicates that a Leyvraz-Ullmo distribution is not sufficient to characterize chaotic tunnelling.

## VII. CONCLUSION

In this paper we have studied in great details the transition between a regular and a chaotic regime of tunnelling within a classical configuration that can be achieved experimentally. We have shown why  $\hbar_{\text{eff}}$  has to be small enough if one wants to reach for the first time the chaotic regime in real systems. In recent experiments with cold atoms, it requires to increase the modulation period up to one order of magnitude (that is at least the MHz).

Theoretically, there is also a lot of work to do if we want to understand and therefore predict the fluctuations quantitatively. The semiclassical regime requires to study carefully the dynamics with complex coordinates. However, the present work has shown clearly that the abrupt transition between a regular and a chaotic regime of tunnelling corresponds to a classical transition that can be identified very precisely. Tunnelling being a relevant concept in a semiclassical regime only, it is therefore not surprising that the future investigations on chaotic tunnelling will have to keep track of the classical dynamics in one way or another.

## Acknowledgments

We acknowledge A. Shudo, S. Tomsovic, D. Ullmo and W. Hensinger for stimulating discussions. A. M. is grateful towards O. Boebion for computer assistance in the

Laboratoire de mathématiques et de physique théorique de Tours and thanks the Laboratoire Kastler Brossel de Paris for kind hospitality. Laboratoire Kastler Brossel de l'Université Pierre et Marie Curie et de l'Ecole Normale Supérieure is UMR 8552 du CNRS. Laboratoire de mathématiques et de physique théorique de l'Université François Rabelais is UMR 6083 du CNRS.

## APPENDIX A: INTEGRAL APPROXIMATION NEAR THE PITCHFORK BIFURCATION

When one classical parameter is smoothly varied in a non-integrable Hamiltonian system, its periodic orbits follow infinite fractal-like cascade of bifurcations through which they cannot be followed smoothly. However, all the bifurcations can be classified according to a simple set of scenarios: for a given bifurcation of a given periodic orbit, the phase-space dynamics of the original parameter-dependent Hamiltonian can be uniformly approximated by an integrable parameter-dependent Hamiltonian which retains the relevant features only. Of course, because one cannot get rid of the chaotic dynamics, this approximation does make sense only locally, that is near the periodic orbit, in the neighborhood of the bifurcation. It is the object of the Hamiltonian normal form theory to classify the bifurcations and obtain the simplest form of the approximated integrable Hamiltonians (the so-called normal forms). Generically, *i.e.* when no constraint or symmetry is present, the one parameter Hamiltonian normal forms have been completely classified by Meyer [30, 44, 45]. However, the bifurcation shown in Fig. 2 is out of the scope of Meyer's classification precisely because the time reversal symmetry plays a key role. Even if the Poincaré surface of section near the origin (see Fig. 2 (b)) cannot be distinguished from the one corresponding to Meyer's transitional bifurcation (see for instance Fig. 9 (b) in [30]), it is crucial to note that, in our case, two *distinct*  $2\pi$ -periodic orbits have emerged from the origin. In a transitional bifurcation, the two stable islands would correspond to the *same*  $4\pi$ -periodic orbit. Therefore they would be classically connected to each other and would be irrelevant for tunnelling. Let us sketch briefly how to obtain the Hamiltonian normal form in our case.

1. The first step is to find the value  $\gamma_0$  of  $\gamma$  at which the bifurcation occurs ( $\theta$  is kept fixed). Such a bifurcation occur when the trace of the monodromy matrix  $M_\gamma$  at the origin after one period is 2 and corresponds in the  $(-2\gamma, 4\gamma\theta)$ -plane to the border of the even Arnold tongues (see Fig. 20.1 in [46]) (the transitional case occurs when  $\text{tr}M_\gamma = -2$  at the border of the odd Arnold tongues). More precisely, the case shown in Fig. 2 corresponds to  $\theta = 1.724137$  (the experimental value in the NIST experiment) and the bifurcation takes place at  $\gamma_0 \simeq 0.564673$ . In the following, we use  $\varepsilon = \gamma - \gamma_0$ .

Let us denote by  $\mathcal{Y}_\varepsilon(z)$  [resp.  $\mathcal{Z}_\varepsilon(z)$ ] the solution of the Mathieu equation

$$y''(x) + (4\gamma\theta + 4\gamma\cos(2x))y(x) = 0 \quad (\text{A1})$$

such that  $\mathcal{Y}_\varepsilon(0) = 0$  and  $\mathcal{Y}'_\varepsilon(0) = 1$  [resp.  $\mathcal{Z}_\varepsilon(0) = 1$  and  $\mathcal{Z}'_\varepsilon(0) = 0$ ]. The prime stands for the derivative with respect to  $x$ . For  $\varepsilon = 0$ , it is straightforward to show that

$$M_{\gamma_0} = \begin{pmatrix} 1 & \frac{1}{4\pi}\mathcal{Z}'_0(\pi) \\ 0 & 1 \end{pmatrix} \quad (\text{A2})$$

where  $\mathcal{Z}'_0(\pi) \simeq 1.480919$  for  $\theta = 1.724137$ .

2. The second step is to make a (linear)  $2\pi$ -periodic canonical change of coordinate that eliminates the time-dependence in the quadratic part of Hamiltonian (2), near the origin and uniformly in  $\varepsilon$ . We are then led to the Hamiltonian

$$\left(-\frac{1}{2}\frac{1}{4\pi}\mathcal{Z}'_0(\pi) + \alpha\varepsilon\right)q^2 + \frac{1}{2}\beta\varepsilon p^2 + \frac{1}{2}\delta\varepsilon p^2 \quad (\text{A3})$$

+higher order  $2\pi$ -periodic terms

where  $\alpha, \beta, \delta$  are  $\varepsilon$ -independent coefficients. Only  $\beta = \frac{1}{\pi}\partial_\varepsilon\mathcal{Y}_\varepsilon(\pi)$  evaluated at  $\varepsilon = 0$  will be relevant since  $\alpha$  and  $\delta$  can be eliminated by a suitable canonical change of coordinates following a method explained in [30, section 4.2]. In our case  $\beta \simeq 2.008/\pi$ . We are therefore led to the following normal form of the quadratic part of the Hamiltonian:

$$\left(-\frac{1}{2}\frac{1}{4\pi}\mathcal{Z}'_0(\pi)\right)q^2 + \frac{1}{2}\beta\varepsilon p^2 \quad (\text{A4})$$

+higher order  $2\pi$ -periodic terms

3. Following the same reasoning that lead to the transitional normal form [30, sections 4.2], all higher order  $2\pi$ -periodic terms, but the resonant terms of the form  $h_k(\varepsilon)p^k$ , can be cancelled by a suitable canonical change of coordinates. Because of the time reversal symmetry, the coefficient  $h_3$  vanishes identically and therefore the leading order normal form is

$$\left(-\frac{1}{2}\frac{1}{4\pi}\mathcal{Z}'_0(\pi)\right)q^2 + \frac{1}{2}\beta\varepsilon p^2 - \frac{1}{4}h_4(0)p^4. \quad (\text{A5})$$

The explicit calculation of  $h_4(0)$  is tedious but it can be estimated numerically by fitting the coordinate  $q = 0, p = \pm\sqrt{\beta\varepsilon/h_4}$  of the satellite  $2\pi$ -periodic orbits for  $\varepsilon > 0$ . We obtain  $h_4 \simeq 0.0320$ .

It is far from obvious that the quantization of the normal form (A5) will give a good approximation of the quasi-energies of the tunnelling doublet. Some discrepancies may rise from the fact that quantum physics is invariant under canonical transformations only at the leading order in  $\hbar$ . When we swap  $p$  with  $q$  and change the sign of the energies, the normal form (A5) leads to a standard 1D double-well problem whose quantum spectrum can be found by numerically diagonalizing the Hamiltonian written in a harmonic basis. The tunnelling splitting of the ground doublet is given by the dotted line in Fig. 7 and it agrees reasonably well with the exact numerical result for  $\gamma$  near  $\gamma_0$ .

- 
- [1] A. Messiah, *Mécanique Quantique (2 vol.)* (Dunod, Paris, 1964), english translation: North-Holland (Amsterdam).
- [2] R. Balian and C. Bloch, *Ann. Physics* **84**, 559 (1974).
- [3] M. Wilkinson, *Physica D* **21**, 341 (1986).
- [4] M. Wilkinson and J. H. Hannay, *Physica D* **27**, 201 (1987).
- [5] in *Chaos et Physique Quantique — Chaos and Quantum Physics*, Les Houches, école d'été de physique théorique 1989, session LII, edited by M. Giannoni, A. Voros, and J. Zinn-Justin (North-Holland, Amsterdam, 1991).
- [6] C. Dembowski, H.-D. H.-D. Gräf, A. Heine, R. Hofferbert, H. Rehfeld, and A. Richter, *Phys. Rev. Lett.* **84**, 867 (2000).
- [7] W. A. Lin and L. E. Ballentine, *Phys. Rev. Lett.* **65**, 2927 (1990).
- [8] O. Bohigas, D. Boosé, R. Egdio de Carvalho, and V. Marvulle, *Nuclear Phys. A* **560**, 197 (1993).
- [9] O. Bohigas, S. Tomsovic, and D. Ullmo, *Phys. Rep.* **223**, 43 (1993).
- [10] S. Tomsovic and D. Ullmo, *Phys. Rev. E* **50**, 145 (1994).
- [11] S. C. Creagh and N. D. Whelan, *Phys. Rev. Lett.* **77**, 4975 (1996).
- [12] O. Brodier, P. Schlagheck, and D. Ullmo, *Ann. Physics* **300**, 88 (2002).
- [13] J. Zakrzewski, D. Delande, and A. Buchleitner, *Phys. Rev. E* **57**, 1458 (1998).
- [14] A. Mouchet, C. Miniatura, R. Kaiser, B. Grémaud, and D. Delande, *Phys. Rev. E* **64**, 016221 (2001).
- [15] W. K. Hensinger, H. Häfner, A. Browaeys, N. R. Heckenberg, K. Helmerson, C. McKenzie, G. J. Milburn, W. D. Phillips, S. L. Rolston, H. Rubinsztein-Dunlop, and B. Upcroft, *Nature* **412**, 52 (2001).
- [16] D. A. Steck, H. O. Windell, and M. G. Raizen, *Science* **293**, 274 (2001).
- [17] W. K. Hensinger, *Experimental tests of quantum nonlinear dynamics in atom optics* (The University of Queensland, Australia, 2002), PhD thesis.
- [18] W. K. Hensinger, A. Mouchet, P. S. Julienne, D. Delande, N. R. Heckenberg, and H. Rubinsztein-Dunlop, *Analysis of dynamical tunnelling experiments with a Bose-Einstein condensate* (in preparation for *Phys. Rev. A*).
- [19] in *Laser and manipulation of atoms and ions*, Enrico Fermi international summer school, Course CXVIII, 9-19 July 1991, edited by E. Arimondo, W. D. Phillips, and F. Strumia (North-Holland, Amsterdam, 1992).
- [20] R. T. Lawton and M. S. Child, *Molecular Phys.* **44**, 709 (1981).
- [21] E. L. Sibert, W. P. Reinhardt, and J. T. Hynes, *J. Chem. Phys.* **77**, 3583 (1982).
- [22] M. E. Kellman and E. D. Lynch, *J. Chem. Phys.* **87**, 5386 (1987).
- [23] J. P. Rose and M. E. Kellman, *J. Chem. Phys.* **105**, 7348 (1996).
- [24] E. J. Heller, *Nature* **412**, 33 (2001).
- [25] A. Mouchet and D. Ullmo, *Physics World* **14**, 24 (2001).
- [26] B. Goss Levi, *Physics Today* **54**, 15 (2001).
- [27] J. Heading, *An Introduction to Phase-Integral Methods* (Methuen, John Wiley and sons, Inc., London, New York, 1962).
- [28] M. J. Davis and E. J. Heller, *J. Phys. Chem.* **85**, 307 (1981).
- [29] M. Kuś, F. Haake, and D. Delande, *Phys. Rev. Lett.* **71**, 2167 (1993).
- [30] P. Lebœuf and A. Mouchet, *Ann. Physics* **275**, 54 (1999).
- [31] A. Shudo and K. S. Ikeda, *Physica D* **115**, 234 (1998).
- [32] S. Tomsovic, *J. Phys. A* **31**, 9469 (1998).
- [33] in *Tunneling in complex systems*, Vol. 5 of *Proceedings from the Institute for Nuclear Theory*, edited by S. Tomsovic (World Scientific Publishing, Singapore, 1998).
- [34] V. Averbukh, N. Moiseyev, B. Mirbach, and H. J. Korsh, *Z. Phys. D* **35**, 247 (1995).
- [35] N. W. Ashcroft and N. D. Mermin, *Solid State Physics* (Saunders College, Philadelphia, 1976).
- [36] K. Husimi, *Proc. Phys. Mat. Soc. Japan* **22**, 264 (1940).
- [37] M. Greiner, O. Mandel, T. Esslinger, T. W. Hänsch, and I. Bloch, *Nature* **415**, 39 (2002).
- [38] W. K. Hensinger, B. Upcroft, N. R. Heckenberg, G. J. Milburn, and H. Rubinsztein-Dunlop, *Phys. Rev. A* (3) **64**, 063408 (2001).
- [39] R. Luter and L. E. Reichl, *Phys. Rev. A* (3) **66**, 053615 (2002).
- [40] W. H. Zurek, *Nature* **412**, 712 (2001).
- [41] N. L. Balazs and A. Voros, *Ann. Physics* **199**, 123 (1990).
- [42] O. Brodier, P. Schlagheck, and D. Ullmo, *Phys. Rev. Lett.* **87**, 064101 (2001).
- [43] F. Leyvraz and D. Ullmo, *J. Phys. A* **29**, 2529 (1996).
- [44] K. R. Meyer, *Trans. Amer. Math. Soc.* **149**, 95 (1970), reprinted in [47].
- [45] K. R. Meyer and G. H. Hall, *Introduction to Hamiltonian Dynamical Systems and the N-Body Problem*, Vol. 90 of *Applied Mathematical Sciences* (Springer-Verlag, New York, 1992).
- [46] M. Abramowitz and I. A. Segun, *Handbook of mathematical functions* (Dover publications, New York, 1965).
- [47] R. S. Mackay and J. D. Meiss, *Hamiltonian Dynamical Systems* (Adam Hilger, Bristol and Philadelphia, 1987).